

Benzene Physical and Chemical Organogels: Effect of Network Scaffolding on the Thermodynamic Behavior of Entrapped Solvent Molecules

Nov Marković, Milena Ginić-Marković, Naba K. Dutta

Ian Wark Research Institute, ARC Special Research Centre, University of South Australia, Mawson Lakes Boulevard, Mawson Lakes SA 5095, Australia

Received 26 October 2002; accepted 12 June 2003

DOI 10.1002/app.21059

Published online in Wiley InterScience (www.interscience.wiley.com).

ABSTRACT: This paper presents a thermodynamic investigation of the benzene physical and chemical organogels, using differential scanning calorimetry (DSC) and intends to draw an appropriate relationship between the gel network structure and the properties. Physical gels, formed by an aluminium soap of fatty acid, and chemical gels, created by *in situ* cross-linking of a siloxane copolymer are investigated. The effects of the type and quantity of the gelators and their corresponding network mesh size distribution in the gels on crystallization, melting, and their kinetics are examined. It appears that the kinetics of crystallization of the entrapped solvent is significantly affected by the quality of the gel network scaffolding and can be treated successfully by the

Avrami equation of crystallization. From the melting behavior of the entrapped solvent crystallites, quantitative information about the number of solvent molecules bound per molecule of the gelator has been extracted. DSC proves to be a reliable technique to evaluate the population distribution of solvent molecules trapped in the physical and chemical organogel network scaffolding. The state of the solvent may be treated as a probe to understand the structure of the gels. © 2004 Wiley Periodicals, Inc. *J Appl Polym Sci* 94: 1253–1264, 2004

Key words: organogels; nucleation; differential scanning calorimetry (DSC); crystallization; network scaffolding; self-organization

INTRODUCTION

The hierarchical self-assembly and gelation are areas of increasing interest due to their importance in polymer technology, biotechnology, food technology, pharmacology, controlled release applications, surfactant industries, etc. Significant research effort has been dedicated to the hydrogel networks that are hydrophilic and can be swollen by water, particularly for biopolymers in food, pharmaceutical, agricultural, medicinal, and similar industries.^{1–3} By considering the structural features of proteins and their functions, various amphiphilic copolymers have been designed and synthesized to develop self-assembly systems especially in water.⁴ Their inter-macromolecular self-associations, nanoparticle formation, pH and temperature sensitivity, and rheological behavior have been investigated in detail.^{5–9} On the contrary, very little attention has been focused on organogels in the past and is an area of increasing recent interest.^{10–12}

The importance of organogels in everyday life has increased as it is realized that application of small quantities of suitable single or multicomponent gel-

ing agents exhibit the ability to gel a vast quantity of solvents or fuels.¹³ Such gels could be formed either by physical thermoreversible aggregation (physical gel) or by entrapment of liquid in a chemical network structure (chemical gels). Design and synthesis of new and simple organogelator has received significant recent attention. A large number of organogelators of different categories has been identified in recent years by different investigators.^{14–22} Physical gel formation can generally be best understood as resulting from competition between tendencies of the gelator to dissolve in the solvent and tendencies for it to self-assemble.^{23–31} From the limited studies made on thermoreversible organogels using a variety of techniques, including neutron and X-ray scattering, optical, fluorescence and atomic force microscopy, spectroscopic and calorimetric investigations, so far no generalization on the thermodynamic behavior of the gels could be made, as it is dependent on the individual gelator-solvent system.^{32–35} The nature of the solvent changes the ratios of inter- and intramolecular bonds and exerts a substantial effect on the structure and elastic properties of the gels.

Besides physical gelators, specially formulated *in situ* cured polymers have emerged as potential chemical gelators with relatively simple application procedures. There is a vast amount of literature on cross-linked network polymers, but it is only recently that

Correspondence to: N. K. Dutta (Naba.Dutta@unisa.edu.au).

TABLE I
Formulations of Benzene Physical and Chemical Organogels

| Formulation | Physical gels | | Formulation | Chemical gels | | |
|-------------|--------------------|-----------------------|-------------|-----------------------|-----------------------|---------------|
| | Soap (S) (% wt) | Benzene (B) (% wt) | | Benzene (B) (% wt) | Copolymer A (% wt) | DVB (% wt) |
| B100 | 0 | 100 | B100 | 100 | 0 | 0 |
| PS2B | 2 | 98 | C50B | 90.6 | 5.7 | 3.7 |
| PS10B | 10 | 90 | C30B | 85.3 | 8.9 | 5.8 |
| PS15B | 14 | 86 | C20B | 79.5 | 12.4 | 8.1 |
| PS30B | 25 | 75 | C10B | 66 | 20.6 | 13.4 |
| PS37B | 29 | 71 | C0 | 0 | 60.5 | 39.5 |
| ALSP100 | 100 | 0 | — | — | — | — |

an attempt has been directed to confine large amounts of solvent using chemical gel networks.^{36–39} It is well known that the swelling of a preformed network polymer with a solvent results in a network with different physical properties compared to a network polymer actually polymerized (or cross-linked) *in situ* in the solvent.^{40–43} The key point remains that changing the reaction conditions, namely the proportion of reagents, the addition of catalyst, and reaction temperature could change the properties of cross-linked polymer networks dramatically.^{44,45}

Thermodynamic and kinetic investigation can provide much in-depth information into the gel network structure formation and mechanism, however, only limited research on hydrocarbon-based gels has been published. Recently, we have shown that the state of the solvent in gel network scaffolding may be used as a probe to understand the structure of the gels.⁴⁶ The aim of this research is to investigate the thermodynamic behavior of benzene organogels to achieve fundamental understanding of the relationship between the gel network scaffolding and the gel properties.

EXPERIMENTAL

Ingredients

The hydrocarbon used for this investigation is benzene: CAS No [71-43-2], molecular formula/weight of C_6H_6 / 78 g mol⁻¹, T_b 80.2°C, T_m +5.5°C, density 0.879 g ml⁻¹, and dielectric constant of 2.2.⁴⁷ Benzene was purchased from Aldrich chemicals and was used without further purification. The organogelator used for physical gels is the commercially available gelling agent, Calford G-760TM, (ALSP) Blachford, Canada.

Organogelator copolymer A, used for chemical gelation, was prepared by copolymerization of linear poly[(hydrogen methyl) siloxane] or D₃₃ (degree of polymerization 33), with octamethyl cyclosiloxane (D₄), using a ring-opening acid catalyzed reaction. Both D₄ and D₃₃ were obtained from Dow Corning Corporation, USA. Solvent THF used for dilution of Pt-catalyst (Pt-divinyl tetra methyl-di siloxane, Gelest,

USA, used for chemical gels) was distilled and dried before use.

Preparation of gels

Both physical and chemical types of organogels were obtained in an identical manner by adding the specified quantities of ingredients into a known volume of benzene and mixing them thoroughly using a mechanical stirrer. After initial mixing, the reaction was left for completion in tightly closed containers for ~ 24 h prior to further tests. All preparations were performed at ambient temperature. The gels formed could be readily detected by failure of the gelled mixture to flow. The detail formulations and their designations for benzene-based physical (P) organogels are presented in Table I.

In the chemical gels the components were: copolymer A, cross-linker divinylbenzene (DVB), and the hydrocarbon of interest. If copolymer A and cross-linker DVB were mixed together with different quantities of benzene, no reaction occurred. To initiate the cross-linking reaction, a suitable catalyst was necessary, and Pt-complex was found to be the most effective at ambient temperatures. The cross-linking reaction of copolymer A with DVB was initiated by addition of Pt-catalyst (quantity in order of ppm). In this reaction of cross-linking (also known as hydrosilylation) ratios between copolymer A and DVB were always kept the same and their formulations are presented in Table I. Generally, critical parameters controlling the gelation using chemical organogelators are: quantity of gelator and cross-linker, temperature of the reaction, quality of hydrocarbon/solvent, and type of catalyst used. The *in situ* reaction and gelation was monitored by evaluation of the gel point by FTIR, low oscillation rheology, and measurements of cross-link density of the so-obtained gel networks and discussed elsewhere.⁴⁸

Instrumentation

DSC was carried out using a TA Instrument DSC 2920. The instrument was calibrated for cell constant and base-

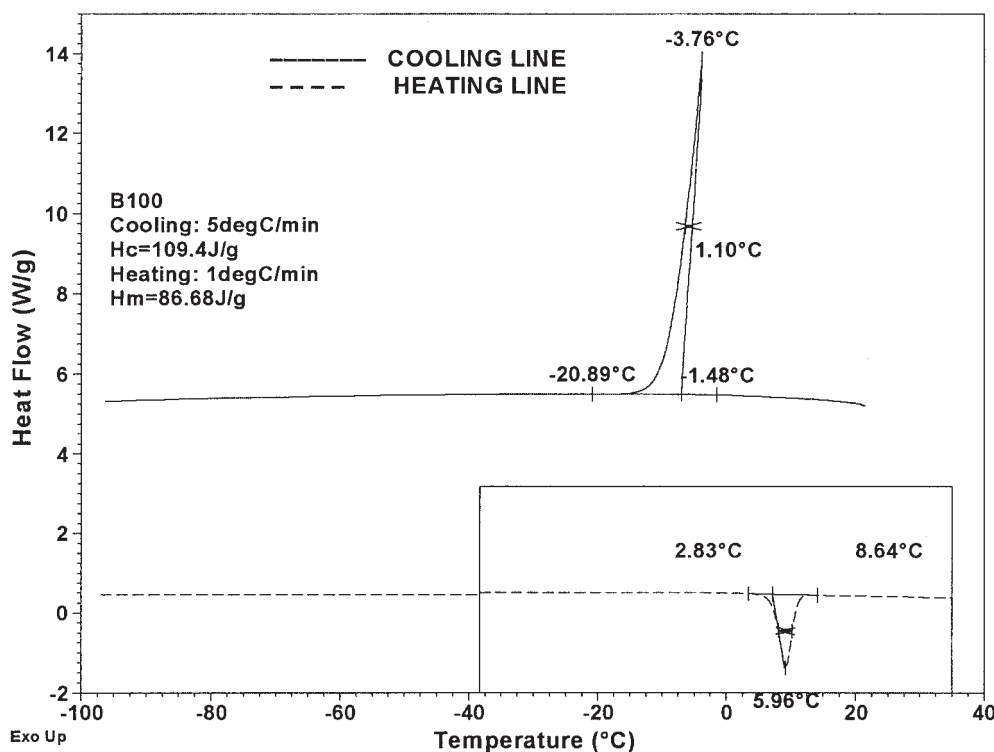


Figure 1 Crystallization and melting behavior of pure solvent benzene (B100) with cooling rate $5^{\circ}\text{C min}^{-1}$ and heating rate of $1^{\circ}\text{C min}^{-1}$.

line with identical experimental conditions as used for the experimental samples. A weighed amount of sample (quantity between 6 and 10 mg) was placed in hermetically sealed Al-pans, to avoid the leakage of solvent and other volatile ingredients. The furnace was constantly purged with nitrogen with a flow of 50 ml min^{-1} . In a typical temperature program the samples were cooled from room temperature to the desired temperature (normally to -100°C) with a cooling rate of $5^{\circ}\text{C min}^{-1}$. After reaching the desired low temperature, samples were held isothermally at that temperature for 5 min (isotrap segment) to complete crystallization. Subsequently, the samples were heated linearly with ramp of $1^{\circ}\text{C min}^{-1}$ up to 100°C (scan rate was very low to approach the equilibrium). Experiments with different scanning rates were also carried out to understand the kinetics of the crystallization/melting process.^{49,50} After runs were completed the weight of the sample was checked and if the weight agreed with initial weight within 5% the run was accepted as valid. All runs were performed in triplicate with standard error not exceeding 8% in total.

RESULTS AND DISCUSSION

Dependence of crystallization behavior on gel network structures

Figure 1 shows the typical DSC traces for the pure solvent benzene during cooling (at a rate of $5^{\circ}\text{C min}^{-1}$)

from melt and subsequent heating (at the rate of $1^{\circ}\text{C min}^{-1}$). The characteristic crystallization (cooling curve) and melting peaks (heating curve) are clearly observed for benzene with the distinctive peak temperatures. The crystallization and melting behavior may be characterized by the heat of crystallization (ΔH_c), heat of fusion (ΔH_m), the peak temperatures (T_c , T_m), and the peak width at the half height. From Figure 1 the melting temperature of the solvent crystals at $+5.96^{\circ}\text{C}$ is clearly evident and is in good agreement with the literature values.⁵¹ Also in the same figure limit temperatures, peak maxima as well as peak width at the half peak height for both crystallization and melting are recorded. The same methodology for extracting the same parameters has been introduced for all benzene physical and chemical gels.

DSC thermograms were also performed for all the pure raw ingredients used for both physical and chemical gelation (physical gelator ALSP, monomer D₃₃, chemical gelator co-polymer A as well as crosslinker DVB) using identical experimental conditions. From the DSC traces obtained no significant crystallization/melting enthalpy could be observed.⁴⁶ Therefore, the effect of gel network scaffolding on the crystallization/melting behavior of the solvents entrapped in the gels can provide in-depth understanding on the state of the solvent molecules within the gel network structure and mechanism of gelation. The enthalpy for

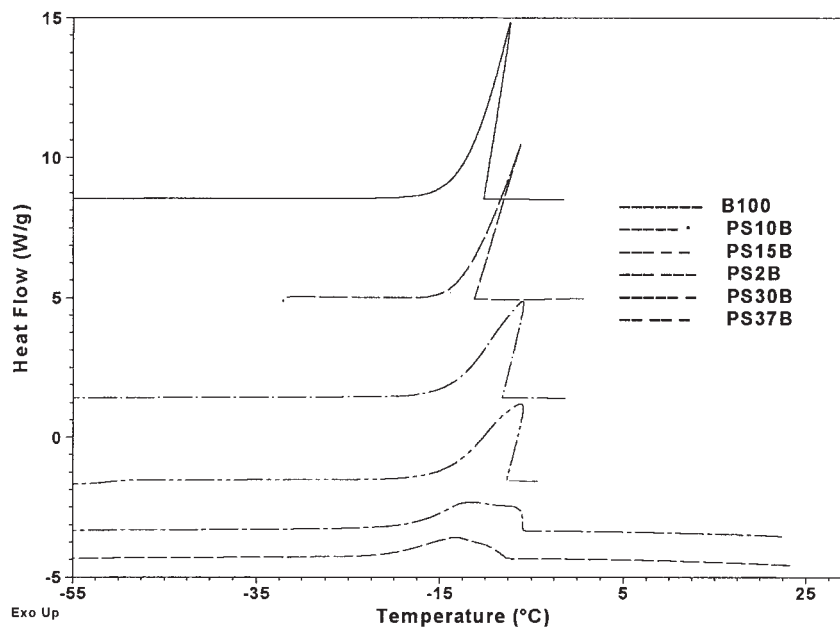


Figure 2 Summary of the crystallization exotherms for benzene physical organogels.

pure solvent benzene, ΔH , was considered as 100% free solvent and used for calculations of the number of bound benzene molecules (α molecules) entrapped within network.

Figure 2 illustrates the cooling DSC traces of benzene physical gels with different levels of gelling agents, ALSP (Table I). The DSC thermogram of pure solvent benzene without gelator is also shown in the graph, which is sharp and corresponds to the crystallization of the free solvent. The substantial change in the nature of the solvent crystallization phenomenon, associated with peak shift, peak widening, and decrease in enthalpy with increase in concentration of gelator ALSP, is clearly evident from the figure. The beginning (start), peak (T_c), and end of crystallization exotherm (stop) are derived from the DSC thermograms and the details are given in Table II.

The difference in the benzene crystal structure formation with increase in the concentration of gel-

ling agent ALSP is apparent from the cooling DSC traces. The thermograms of the gels exhibit a single relatively broader exothermic peak compared with pure benzene (Fig. 1). A progressive increase in peak width, concomitant with decrease in peak height is observed with increased gelator level. A systematic shift in peak temperature T_c toward lower values with an increase in gelator is also evident (from -3.8 to -13.2 °C) (Fig. 2, Table II). The shift of the crystallization temperature of the confined solvent to lower values has also been reported by other investigators⁵²⁻⁵⁴ in the case of *n*-hexane and heptane in elastomer gels. It has been demonstrated that the T_c of the solvent confined in the gel is directly related to the radius of the pore of the mesh of the gel network structure ($R_p = -a/\Delta T + b$, where $\Delta T = T_0 - T$; T_0 is the triple point temperature of solvent and a and b are two constants depending on the solvents). In the case of

TABLE II
Summary of Crystallization and Melting Data for Benzene Physical Organogels

| Sample | | Crystallization parameters | | | | Melting parameters | | | |
|-------------|----------------|----------------------------|-----------|-----------------|------------|--------------------|-----------|-----------------|------------|
| Designation | Benzene (% wt) | Start (°C) | Stop (°C) | Peak width (°C) | T_c (°C) | Start (°C) | Stop (°C) | Peak width (°C) | T_m (°C) |
| ALSP100 | 0 | — | — | — | — | — | — | — | — |
| PS37B | 71 | -7.2 | -29.9 | 8.5 | -13.2 | -5.9 | 8.8 | 3.4 | 4.8 |
| PS30B | 75 | -5.5 | -23.7 | 9.6 | -11.4 | -6.5 | 8.4 | 3.3 | 5.0 |
| PS15B | 85 | -5.6 | -22.3 | 4.0 | -6.2 | -1.0 | 9.1 | 3.0 | 5.8 |
| PS10B | 90 | -7.5 | -19.9 | 3.2 | -5.9 | -5.9 | 10.5 | 3.1 | 6.8 |
| PS2B | 98 | -6.2 | -21.9 | 4.6 | -4.5 | 1.6 | 8.7 | 2.3 | 6.2 |
| B100 | 100 | -1.5 | -20.6 | 1.3 | -3.8 | 2.8 | 8.6 | 1.2 | 5.9 |

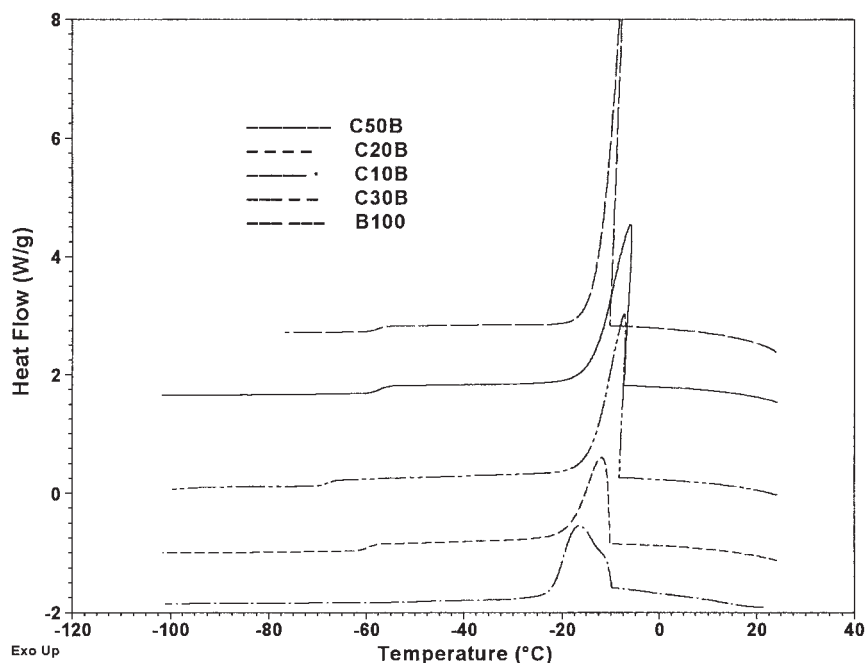


Figure 3 DSC thermogram of the dynamic cooling crystallization of benzene chemical gels: effect of concentration of gelling agent.

benzene physical gels investigated, the peak broadening rather than appearance of distinct new crystallization peak/s for the confined solvent indicates that solvent benzene has heterogeneity in distribution of confinement. Therefore, there is broadness in the distribution of the mesh size of the pore in the gel network scaffolding.

Figure 3 reveals the cooling DSC traces of benzene chemical gels with different levels of copolymer A gelling agent (formulations also given in Table I). With an increase in gelator A level, a similar trend, as observed in the case of physical gels, is also recognized. The crystallization peak shifts to the lower temperature, the exothermic peak becomes broader, enthalpy of crystallization decreases concomitantly with a wider distribution of the crystal formation. The details of the peak position, width, and crystallization enthalpies are given in Table III.

Properties and quality of solvent entrapped within gel network

The variation in crystallization enthalpies of the trapped solvents in the presence of gelling agent yields important information about the physicochemical processes that govern the behavior of the gel systems. In Figure 4 the enthalpy of crystallization (ΔH_c) for benzene physical and chemical gels has been plotted against the weight percent of solvent present in both types of organogels to evaluate their quality of entrapment. The enthalpy of crystallization of benzene physical and chemical gels shows a negative deviation from linearity. This behavior reveals that the total amount of solvent that is confined in the gel network scaffolding does not crystallize. The dashed line represents 100% free solvent. The higher negative deviation is related to the higher quantity of bound solvent

TABLE III
Melting and Crystallization Parameters for Benzene Chemical Organogels

| Sample | | Crystallization parameters | | | | Melting parameters | | | |
|-------------|----------------|----------------------------|-----------|------------|------------|--------------------|-----------|------------|------------|
| Designation | Benzene (% wt) | Start (°C) | Stop (°C) | Peak width | T_c (°C) | Start (°C) | Stop (°C) | Peak width | T_m (°C) |
| C0 | 0 | — | — | — | — | — | — | — | — |
| C10B | 66 | -9.5 | -25.0 | 8.6 | -16.4 | -13.0 | 3.1 | 4.6 | 1.6 |
| C20B | 79 | -9.3 | -25.6 | 5.2 | -11.8 | -10.1 | 5.5 | 4.4 | 3.4 |
| C30B | 85 | -7.3 | -23.2 | 3.5 | -7.3 | -5.0 | 5.5 | 3.1 | 3.8 |
| C50B | 91 | -6.8 | -20.7 | 3.9 | -6.9 | -3.3 | 7.2 | 2.9 | 4.6 |
| B100 | 100 | -1.5 | -20.6 | 1.3 | -3.8 | 2.8 | 8.6 | 1.2 | 5.9 |

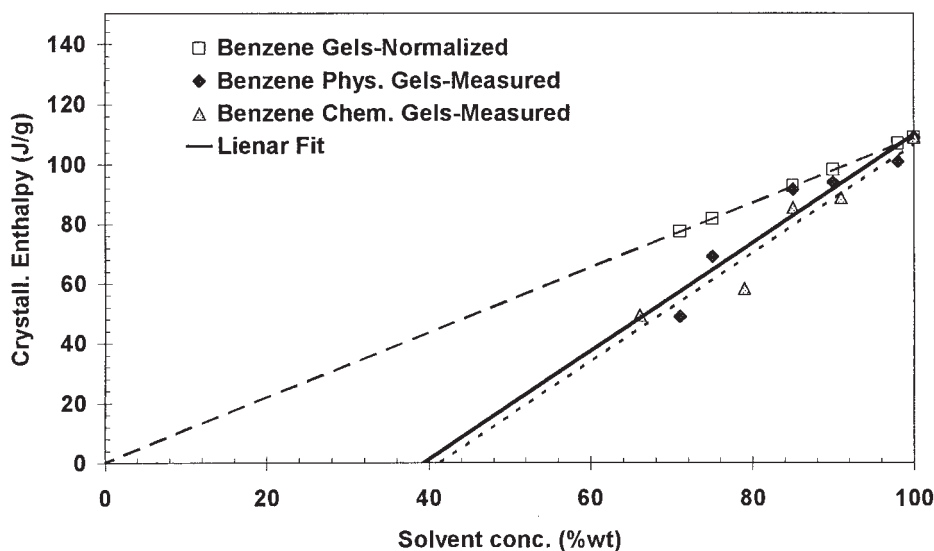


Figure 4 Observed ΔH_c as a function of percent solvent benzene entrapped in the gel network scaffolding.

entrapped within gel network scaffolding that is not crystallizable. A very close range of deviations at each concentration of solvent, regardless of the type of the gels, indicates that the effect of gelation on the molecular dynamics of the solvent molecules is independent of the types of gel network scaffolding.

The hydrated polymer systems have been widely investigated using DSC and various populations of the water fraction depending on the water-polymer interaction have been identified.^{55,56} For pure solvent the large ΔH_c observed may be ascribed to the crystallization of 100% bulk/free solvent. In the case of the gels the exotherms may be ascribed to the crystallization of only the total freezing solvent in the gel. The total solvent content, S_t in the gels may be given by

$$S_t = S_f + S_{fb} + S_{nf} \quad (1)$$

where S_f , S_{fb} , and S_{nf} are the freezing bulk, the freezing-bound, and the non-freezing-bound solvent content, respectively. The quantity of solvent, whose melting/crystallization is not significantly different from those of the bulk solvent, may be called free solvent. Those solvent species exhibit a large difference in transition enthalpies and temperature from the bulk, or those for which no phase transition can be detected calorimetrically may be referred to as bound solvent. It is frequently impossible to observe crystallization exotherms or melting endotherms for the solvent fraction, which is very closely associated with the gelator matrix. This solvent fraction may be designated as non-freezable bound solvent. Thus, the enthalpy of crystallization in the gels may be considered to be consisting of three contributions, and total ΔH_t may be written as

$$\Delta H_t = w_f \Delta H_f + w_g \Delta H_g + w_{fb} \Delta H_{fb} \quad (2)$$

where ΔH_f is the contribution of the free solvent, ΔH_g is the contribution of the gelator, ΔH_{fb} is from the freezing-bound solvent, and w_n are corresponding weight fractions. In the case considered here the contribution of gelator is zero, since at the temperature region of interest the gelators do not crystallize. It is evident from Figure 4 that the nonfreezing solvent progressively increases with an increase in gelator concentration.

Kinetics of crystallization: effect of gel network structure

The temperature and pressure, among all other experimental conditions, are the principal factors in determining the state of any substance: solid, liquid, or gaseous. Usually the former has a more dominant effect than the latter. With heating substance can melt or boil and discontinuity in the volume, temperature, enthalpy related to changes, and heat capacity are identified as a signature of the phase change. These changes take place at a constant temperature and are reported as characteristic phase or first order transitions. In case of crystalline and semicrystalline materials, the shape of the heat of crystallization peak in DSC is directly related to the kinetics (time and temperature dependence) of crystallization. Crystallization is a two-step process, where crystal growth (step 2) takes place at nucleation sites whose appearance (step 1) is controlled by both time and temperature. For isothermal crystallization, the most popularly used equation is

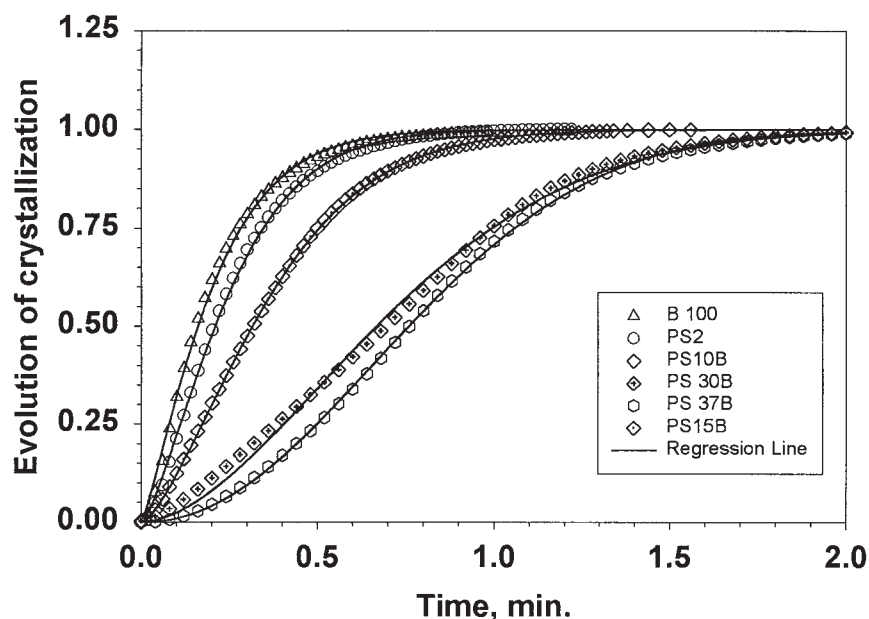


Figure 5 Calculation of Avrami parameters for benzene physical organogels.

$$(1 - X_t) = \exp(-kt^n) \quad (3)$$

where $(1 - X_t)$ is the fraction of the crystallizable polymer not yet crystallized at the time, t and k is the crystallization rate constant related to the number of nuclei per unit volume, the rate of their formation, and crystal geometry.^{57,58} The Avrami exponent, n , represents the nucleation and growth dimension and depends on the type of nucleation and growth process. Equation (3) was independently derived by a series of authors and is popularly known as the Avrami equation.^{59–63}

Many investigators have used successfully Avrami's expression to model nonisothermal crystallization.^{64–66} Particularly, it is useful for systems with a very high rate of crystallization (subject of this investigation), where isothermal crystallization experiments are very difficult to perform precisely. The evolution of the relative crystallinity of the different benzene physical and chemical gels is illustrated in Figures 5 and 6, respectively. The solid lines in both plots represent the predictions obtained using Avrami's eq. (3). An excellent convergence between the experimental and predicted values for both benzene gels clearly indicates that the model equation is appropriate to describe the nonisothermal crystallization kinetics of the experimental benzene gels. Nonlinear regression analyses fitting eq. (3) to the experimental data were carried out using the statistical software Sigmastat/Sigmaplot, SPSS, Chicago, IL. The software uses the Marquardt–Levenberg algorithm to find the coefficients of the variables that give the best fit between the equation and the experimental data. This

algorithm seeks the parameter values that minimize the sum of the squared differences between the observed and predicted values of the dependent variables by an iterative process, until convergence with a predefined tolerance is obtained. The correlation coefficient R^2 for the regression was > 0.99 . From the simulation the best set of kinetic parameters, k and n for the crystallization of solvent molecules in the gels were determined and listed in Table IV for both benzene physical and chemical organogels.

The most important parameter, exponent n , provides qualitative information about the nucleation mechanism and growth process. The n value of close to 1 for bulk solvent benzene indicates primarily one-dimensional homogenous crystal growth (radiating array of rod-like fibrils) (Table IV). The fraction values of n for all the benzene physical gels are in the range of $1 < n \leq 2$, indicating a heterogeneous nucleation with 1-dimensional growth-units.⁶⁷ The value of $n = 1$ indicates rod-like growth from instantaneous nuclei and $n = 2$ indicates rod-like growth from sporadic nuclei. It is clearly observed that the n value systematically increases between 1.26 to 2.0 as the gelator concentration increases and become sporadic ($n = 2$) at very high gelator levels. In comparison to benzene, *cis*-decalin and its gels showed on n value of $3 < n < 4$, indicating three-dimensional spherulitic growth units.⁴⁶ The crystallization growth process depends primarily on the bulk material investigated, however, the gelator concentration appears to introduce inhomogeneity in the nucleation and distribution in crystal size.^{68,69} Based on the Avrami equation and values of n , Sharples⁷⁰ presented a summary table that could

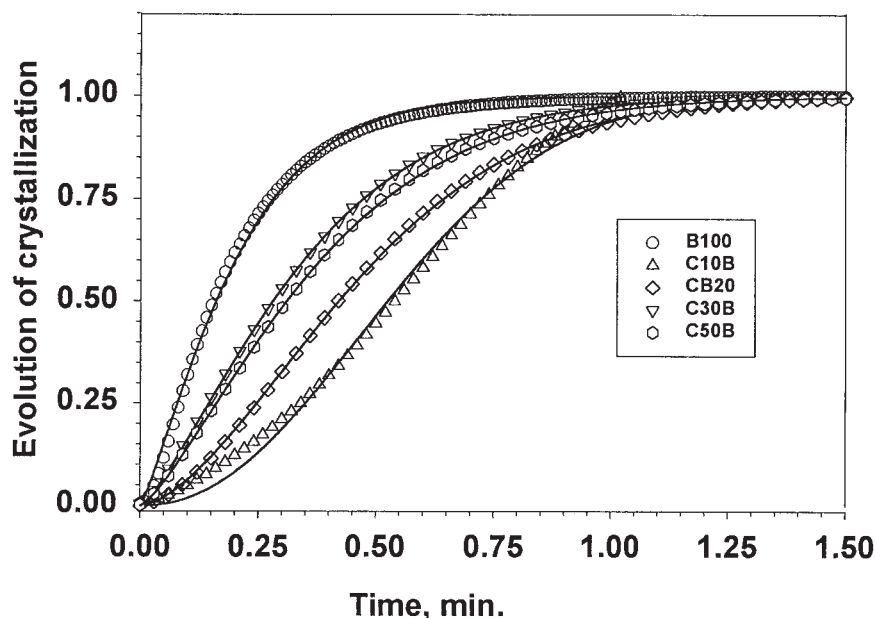


Figure 6 Evolution of the relative crystallinity of chemical benzene gels. The solid lines represents the fitted line using the Avrami equation.

explain different crystallization patterns regarding their nucleation model and growth. In a recent review Sajkiewicz⁷¹ compared crystallization behavior between polymers and low molecular weight materials and confirmed that for the later the steady-state rate of nucleation is reached without any time lag of isothermal crystallization.

The values of k listed in Table IV should be considered to be an average value over a certain temperature range as the rate constant may vary with the temperature. Avrami's rate constant, k , depends on nucleation and growth-rate constants and in principle provides a qualitative check on the course of crystallization. Growth rate is a characteristic of the material investigated and depends on crystallization temperature. If it is assumed that growth rate is not influenced by the nucleation, Avrami's constant may be used to compare the nucleating ability. It is clearly observed from Table IV that increased physical gel network scaffolding significantly decreases the nucleation abil-

ity of hydrocarbon benzene (rate change from 6.55 to 1.24 min^{-n}).

In the case of benzene chemical gels with freezable solvent, the n values were observed to be in the range of $1 < n \leq 2$, similar to the physical gels, indicating predominantly heterogeneous nucleation with one-dimensional growth. The k values in these gels were also decreasing systematically (from 6.55 to 2.80 min^{-n}) with an increase in network scaffolding. Therefore, irrespective of the type of the gel network scaffolding, crystallization of benzene occurs in a one-dimensional fibrillar pattern, however, the nucleation becomes increasingly heterogeneous with increased gelator concentration; and finally, at very high concentrations of gelator, it becomes sporadic in nature.

Kinetics of melting: effect of gel network structure

In Figures 7 and 8 the DSC thermograms of the gel fusion for benzene physical and chemical gels, with

TABLE IV
Avrami's Exponent (n) and Avrami's Constant (k) for Benzene Physical and Chemical Organogels

| Benzene physical gels | | | Benzene chemical gels | | |
|-----------------------|--------------|---------------------------|-----------------------|--------------|---------------------------|
| Designation | Exponent n | k (min^{-n}) | Designation | Exponent n | k (min^{-n}) |
| B100 | 1.22 | 6.55 | B100 | 1.22 | 6.55 |
| PS2B | 1.33 | 5.78 | C50B | 1.33 | 3.33 |
| PS10B | 1.54 | 4.62 | C30B | 1.32 | 3.74 |
| PS15B | 1.46 | 3.77 | C20B | 1.63 | 2.86 |
| PS30B | 1.74 | 1.41 | C10B | 2.16 | 2.80 |
| PS37B | 2.08 | 1.24 | N/A | N/A | N/A |

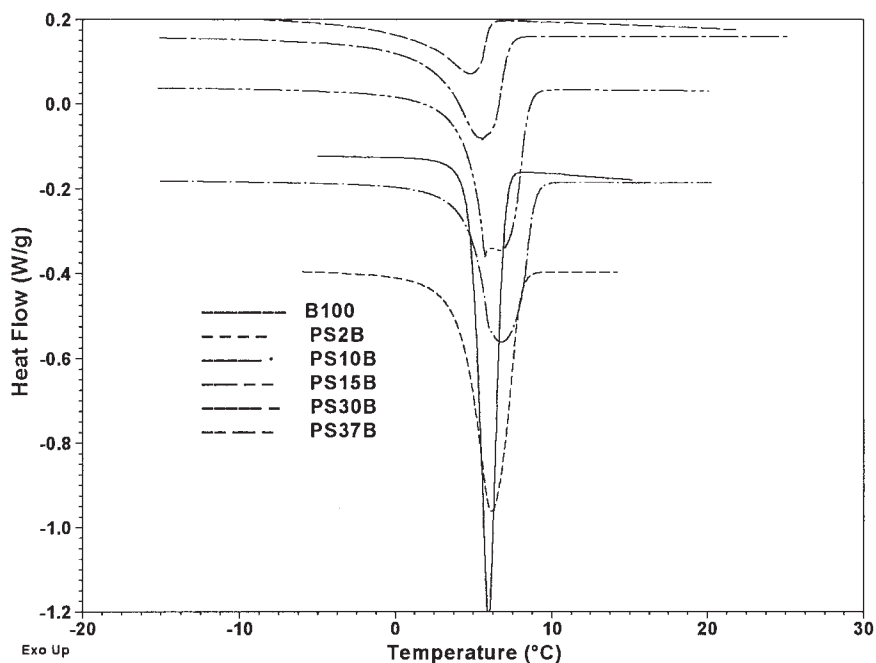


Figure 7 Summary of endothermic peaks of melting for benzene physical organogels.

increasing weight fraction of gelators, are presented. The melting curves of the different experimental gels were obtained at a heating rate of $1^{\circ}\text{C min}^{-1}$. The beginning of melting, peak, and end of melting temperature as well the width at the half height for both physical and chemical organogels are presented in

Tables II and III, respectively. In all the benzene physical gels a single endothermic melting peak is observed and the T_c is not significantly affected by gel network structure. The most concentrated benzene gel sample (PS37B) displayed melting peak of 4.8°C and an insignificant shift compared to benzene itself

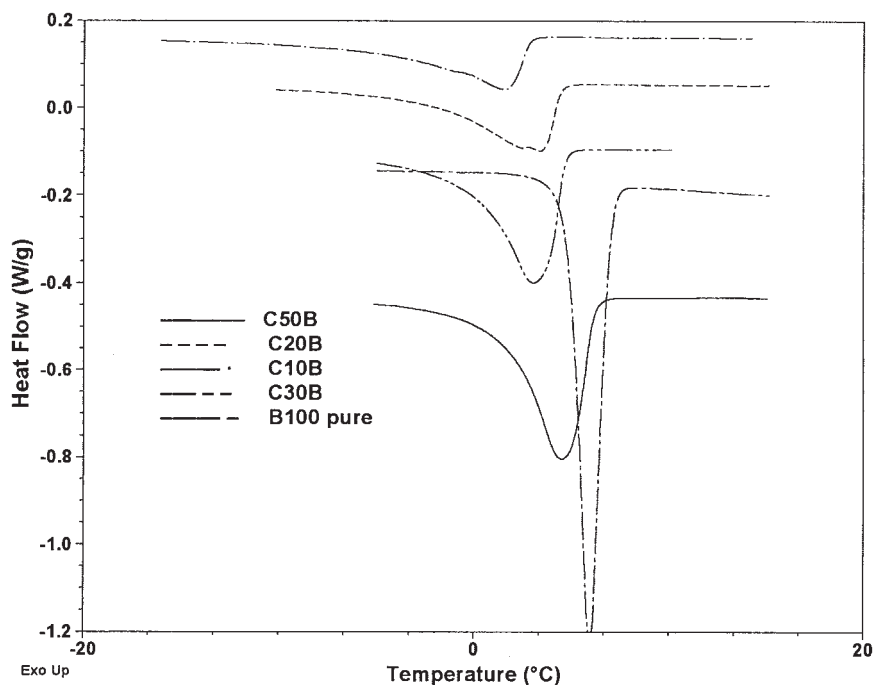


Figure 8 DSC thermogram of the dynamic heating melting endotherm for benzene chemical gels, effect of concentration of gelling agent.

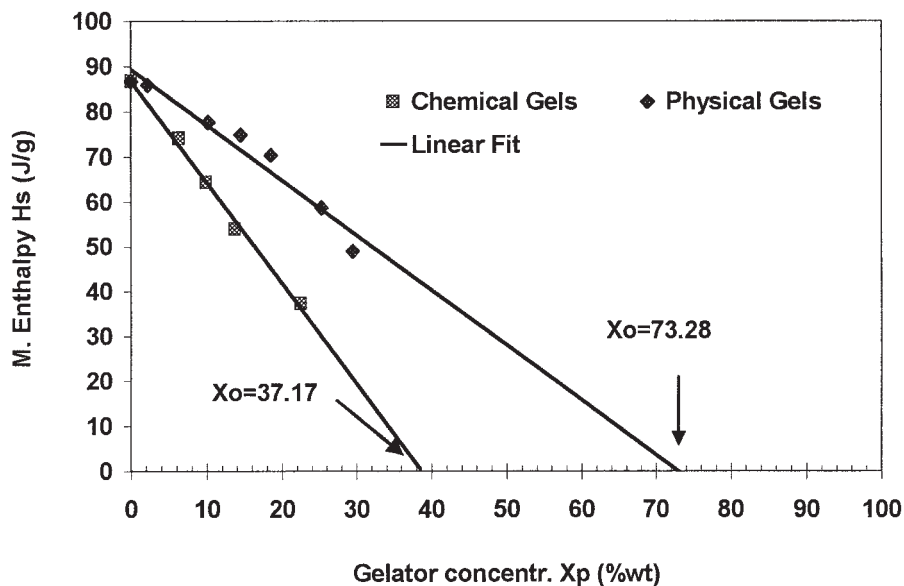


Figure 9 Summary for evaluation of solvent benzene molecules bound to monomer units calculated by extrapolation method for both types of gels.

(5.7°C, B100). However, with an increase in network scaffolding, the broadness of the endotherm progressively increases concomitant with a decrease in peak height; and melting enthalpies associated are significantly different. This observation indicates the increase in the broadness of the distribution of the crystal thickness with an increase in scaffolding, which in turn is attributed to the broadness of the pore size distribution and the quality of the solvent entrapment. A similar observation has also been noted for hydrocarbon gels based on *cis*-decalin.⁴⁶ However, Willemsen et al.¹⁴, using alkyl derivatives of cholic acid as the organogelators, observed an increase in the melting points of the gels with an increase in the concentration of the gelators. The dynamic heating melting endotherm of chemical gels (Fig. 8) showed a similar trend as for the benzene physical gels, except the endotherm peak, T_m , shows a marginal negative shift. The details of the peak characteristics are presented in Table III.

Benzene molecules (α) bound to monomers in physical and chemical gels

The amount of bound solvent in the gels may be calculated from the plot of dependence of their melting enthalpies on the quantity of solvent present using the extrapolation method proposed by several investigators.⁷²⁻⁷⁵ The mathematical model used may be represented as follows:

$$\Delta H_s = \Delta H_{os} \{1 - X_p [1 + \alpha(M_s/M_p)]\} \quad (4)$$

where ΔH_s is the measured solvent enthalpy in the gel system, ΔH_{os} is the melting enthalpy of the pure solvent, X_p is the gelator concentration (wt/wt), M_s and M_p are the solvent and the gelator molecular weights, respectively. Figure 9 illustrates the melting enthalpies as a function of concentrations of gelators for both benzene physical and chemical organogels. An extrapolation of the plot to the zero value of melt enthalpy ($\Delta H_s = 0$) provides information about the number of solvent molecules α bound to monomer molecules using the equation:

$$\alpha = \frac{(1 - X_0)M_p}{X_0M_s} \quad (5)$$

where M_p is the molecular weight of soap ALSP (for physical gels) or monomer D_{33} (for chemical gels) and M_s is the molecular weight of solvent benzene. The value X_0 was calculated by the extrapolation method for both physical and chemical gels, respectively, and is presented in Figure 9.

From Figure 9 the linear dependence between gelator concentration and melting enthalpy for both types of the benzene gels is clearly evident ($R^2 > 98\%$). Extrapolations to zero value of melt enthalpy ($\Delta H_s = 0$) provided values for X_0 of 37.17 for chemical and 73.28 for physical gel respectively. Using eq. (5) it is revealed that almost 3 solvent molecules are bound to each ALSP molecule in benzene physical gels; on the other hand, almost 46 molecules of benzene are bound to the monomer D_{33} of the chemical gels.

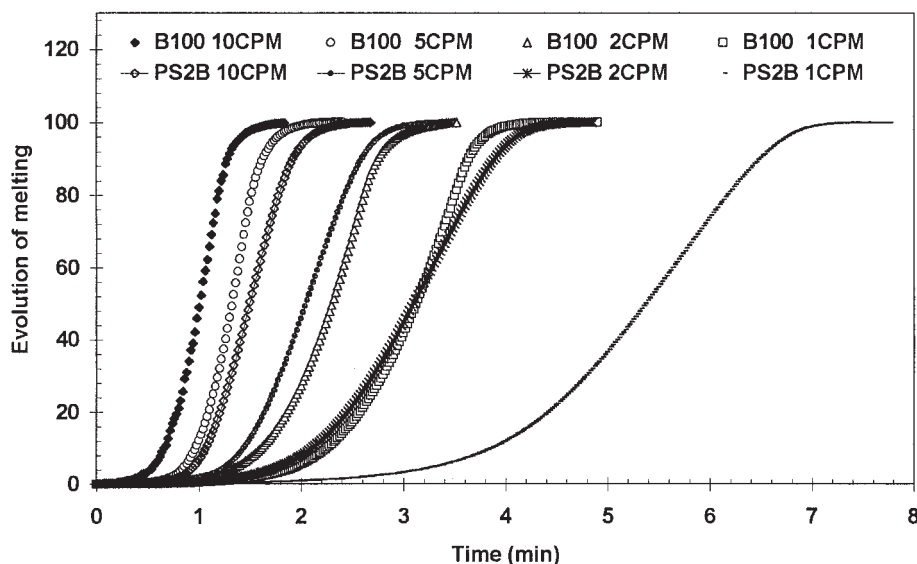


Figure 10 Summary for evolution of melting of the pure benzene (B100) and for physical gel with 2 g ALSP (PS2B) runs with heating ramps of 1, 2, 5, and 10 °C min⁻¹.

Effect of heating rates on dynamics of melting

The evolution of melting of crystallites may depend strongly on the heating rates and were studied in two representative benzene samples using heating rates of 1, 2, 5, and 10 °C min⁻¹. Figure 10 depicts the evolution of melting with elapsed time for pure solvent benzene (B100) as well as for the representative sample of physical gel (PS2B), respectively. It is observed that the melting enthalpies are independent of the heating rate (absolute values are within $\pm 5\%$) within the experimental range. However, with increase in heating rate, the T_m shifted to the higher temperature, which may be considered to be a superheating effect. The rates of melting may be calculated from the slopes of the straight-line portions of the individual plots and are shown in Table V for both samples.

From Table V, an increase in rate of melting with faster heating ramps (from 1 to 10 °C min⁻¹) is clearly evident for both samples. However, if compared to each other at a specific heating ramp, the absolute rates of melting of the trapped benzene crystals within

the gel network scaffolding (PS2B) are slower than the crystals of the bulk/free benzene solvent (B100). This observation confirms that crystallites from solvent molecular species entrapped in gel network scaffolding need higher energy and/or a longer time to melt.

CONCLUSIONS

In this study an investigation of the effect of gel network scaffolding on the population of solvent benzene in the physical and chemical organogels and in turn on the entrapped solvent crystallization, melting, and evaporation is performed using DSC. The extent of crystallization of benzene in the gels, obtained by cooling at constant rate, provides quantitative information about the free, freezable-bound, and non-freezable-bound solvent population in the gels. The nonisothermal kinetic process of nucleation mechanism and its growth are derived using the Avrami equation. The crystallization of neat solvent benzene appears to be primarily homogenous in nucleation and one-dimensional in growth. The heterogeneity in nucleation increases with increased network scaffolding, however, the growth process remains unaffected. From the melting behavior quantitative information about the number of solvent molecules bound per molecule of the gelators has been extracted successfully. The rate of melting of the crystallites entrapped in network scaffolding is slower compared to that of the free crystals.

References

- Dotson, N. A.; Macosko, C. W.; Tirrell, M. In *Synthesis, Characterization and Theory of Polymer Network and Gels*; Aharoni, S. M. Ed.; Plenum Press: New York, 1992.

TABLE V
Summary of Melting Rates for Pure Benzene Solvent (B100) as well as Physical Gel with 2 g of Soap ALSP (PS2B)

| Sample B100 | | Sample PS2B | |
|-------------------------|--|-------------------------|--|
| Heating ramp | Rate of melting (g min ⁻¹) | Heating ramp | Rate of melting (g min ⁻¹) |
| 1 °C min ⁻¹ | 68 | 1 °C min ⁻¹ | 32 |
| 2 °C min ⁻¹ | 88 | 2 °C min ⁻¹ | 48 |
| 5 °C min ⁻¹ | 137 | 5 °C min ⁻¹ | 73 |
| 10 °C min ⁻¹ | 154 | 10 °C min ⁻¹ | 93 |

2. Cohen Addad, J. P. *Physical Properties of Polymeric Gels*; John Wiley & Sons: Chichester, 1996.
3. Meyvis, T. K. L.; De Smedt, S. C.; Demeester, J.; Hennink, W. E. J. *Rheol.* 1999, 43, 933.
4. Dubin, P.; Bock, J.; Davis, R.; Schulz, D. N. Thies, C. Eds.; *Macromolecular Complexes in Chemistry and Biology*. Springer-Verlag: Berlin, 1994.
5. Yamazaki, A.; Song, J. M.; Winnik, F. M.; Brash, J. L. *Macromolecules* 1998, 31, 109.
6. Lee, K. Y.; Jo, W. H.; Kwon, I. C.; Kim, Y-H.; Jeong, S. Y. *Macromolecules* 1998, 31, 378.
7. Nichifor, M.; Lopes, A.; Carpov, A.; Melo, E. *Macromolecules* 1999, 32, 7078.
8. Akiyoshi, K.; Kang, E-C.; Kurumada, S.; Nomura, Y. *Macromolecules* 2000, 33, 6752.
9. Glass, J. E.; Ed.; *Associative Polymers in Aqueous Solutions*: ACS Symposium Series; American Chemical Society; Washington, DC, 1991; Vol. 768.
10. Terech, P.; Weiss, R. G. *Chem Rev* 1997, 97, 3133.
11. Abdallah, D. J.; Weiss, R. G. *Adv Mater* 2000, 12, 1237.
12. Osada, Y.; Kajiwara, K. Eds.; *Gels Handbook*; Academic Press: San Diego, 2001; vols. 1-4.
13. Ishida, H.; Iwama, A. *Combust. Sci. Technol.* 1984, 36, 51.
14. Willemen, H. M.; Vermonden, T.; Marcelis, A. T. M.; Sudholter, E. J. R. *Eur J Org Chem* 2001; 2329 *Langmuir* 2002, 18, 7102.
15. Hanabusa, K.; Matsumoto, M.; Kimura, M.; Kakehi, A.; Shirai, H. *J. Colloid Interface Sci* 2000, 24, 231.
16. Maitra, U.; Potluri, V. K.; Sangeetha, N. M.; Babu, P.; Raju, A. R. *Tetrahedron: Asymmetry* 2001, 12, 477.
17. Geiger, C.; Stanescu, M.; Chen, L.; Whitten, D. G. *Langmuir* 1999, 15, 2241.
18. Amaike, M.; Kobayashi, H.; Shinkai, S. *Bull Chem Soc Jpn* 2000, 73, 2553.
19. te Nijenhuis, K. *Thermoreversible Networks*; *Advances in Polymer Science* Springer-Verlag; Berlin, 1997; vol. 130.
20. Djabourova, M. *Polym Int* 1991, 25, 135.
21. Philippova, O. E.; Chtcheglova, L. A.; Karybians, N. S.; Khokhlov, A. R. *Polym Gels Networks* 1998, 6, 409.
22. Daniel, C.; Deluca, M. D.; Guenet, J. M.; Brulet, A.; Menelle, A. *Polymer* 1996, 37, 1273.
23. Murata, K.; Aoki, M.; Suzuki, T.; Harada, T.; Kawabata, H.; Komuri, T.; Ohseto, F.; Ueda, K.; Shinkai, S. *J Am Chem Soc* 1994, 116, 6664.
24. Lin, Y. C.; Kachar, B.; Weiss, R. G. *J Am Chem Soc* 1989, 111, 5542.
25. Terech, P.; Furman, I.; Weiss, R. G. *J Phys Chem* 1995, 99, 9558.
26. Terech, P.; Ostuni, E.; Weiss, R. G. *J Phys Chem* 1996, 100, 3759.
27. Hanabusa, K.; Tanaka, R.; Suzuki, M.; Kimura, M.; Shirai, H. *Adv Mater* 1997, 9, 1095.
28. Terech, P.; Coutin, A.; Giroud-Godquin, A. M. *J Phys Chem B* 1997, 101, 6810.
29. Placin, F.; Colomes, M.; Desvergne, J. P. *Tetrahedron Lett* 1997, 38, 2665.
30. Inoue, K.; Ono, Y.; Kanekito, Y.; Ishi-i, T.; Yoshihara, K.; Shinkai, S. *Tetrahedron Lett* 1998, 39, 2981.
31. Pozzo, J. L.; Clavier, G. M.; Colomes, M.; Bouas-Laurent, H. *Tetrahedron* 1997, 53, 6377.
32. Spevacek, J.; Saini, A.; Guenet, J. M. *Macromol Rapid Commun* 1996, 17, 389.
33. Loyer, K.; Iliopoulos, I.; Audelert, R.; Olsson, U. *Langmuir* 1995, 11, 1053.
34. Sakai, M.; Sotoh, N.; Tsujii, K.; Zhang, Y. Q.; Tanaka, T. *Langmuir* 1995, 11, 2495.
35. Mal, S. K.; Nandi, A. K. *Langmuir* 1998, 14, 2238.
36. Roberts, K.; Simon, P. G.; Cook, W. D.; Burchill, P. J., *J Polym Sci Part B, Polym Phys* 2000, 38, 3136.
37. Feger, C.; Molis, S. E.; Hsu, S. L.; MacKnight, W. J., *Macromolecules* 1984, 17, 1830.
38. Yildiz, S.; Hepuzer, Y.; Yagci, Y.; Pekcan, O. *Eur Polym J* 2002, 38, 1591.
39. Tanaka, A.; Kago, K.; Nagata, H.; Nitta, K. *Polymer* 2001, 42, 137.
40. Flory, P. J.; Shih, H. *Macromolecules* 1972, 5, 761.
41. Guenet, J. M.; McKenna, G. B. *Macromolecules* 1988, 21, 1752.
42. Rogovina, L. Z. In *Physical Networks*; Burchard, W.; Ross-Murphy, S. B., Eds.; Elsevier: New York, 1990.
43. Hild, G. *Prog Polym Sci* 1998, 23, 1019.
44. Daum, U.; Wei, G.; Luisi, P. L. *Colloid Polym Sci* 1988, 266, 657.
45. Guenet, J. M. *Thermoreversible Gelation of Polymers and Biopolymers*; Academic Press Limited: London, 1992.
46. Markovic, N.; Ginić-Markovic, M.; Dutta, K. N. *Polym Int* 2003, 52, 1095.
47. Whim, B. P.; Johnson, P. G. *Directory of Solvents*; Blackie Academic and Professional: London, 1996.
48. Markovic, N.; Dutta, N.; Williams, D. R. G.; Matisons, J. *Silicon Chem* to appear.
49. Borzacchiello, A.; Ambrosio, L.; Nicholas, C. V.; Purbrick, M. D. *Polym Int* 2000, 49, 122.
50. Haines, P. J. In *Handbook of Thermal Analysis and Calorimetry*, Brown M. E., Ed.; Elsevier: Amsterdam, 1998.
51. Smallwood, M. *Handbook of Organic Solvent Properties*; Arnold; London, 2000.
52. Brun, M.; Lallemand, A.; Quinson, J. F.; Eyraud, C. *Thermochim Acta* 1997, 21, 21.
53. Baba, M.; Gardette, J-L.; Lacoste, J. *Polym Degrad Stab* 1999, 65, 415.
54. Iza, M.; Woerly, S.; Danumah, C.; Kaliaguine, S.; Bousmina, M. *Polymer* 2000, 41, 5885.
55. Nishinari, K. *Colloid Polym Sci* 1997, 275, 1093.
56. Apostolov, A.; Fakirov, S.; Vassileva, E.; Patil, R. D.; Mark, J. E. *J Appl Polym Sci* 1999, 71, 465.
57. Haigh, J. A.; Nguyen, C.; Alamo, R. G.; Mandelkern, L. *J Therm Anal Calor* 2000, 59, 435.
58. Wunderlich, B. In *Thermal Characterization of Polymeric Materials*; Turi, E. A., Ed.; Academic Press: San Diego, 1997; 2nd ed.
59. Goler, V.; Sacks, F.; Sacks, G. *Z Phys* 1932, 77, 281.
60. Kolmogorov, N. *Izv Akad Nauk SSSR, Ser Mater* 1937, 1, 355.
61. Johnson, W. A.; Mehl, K. E. *Am Inst Mining Met Eng* 1939, 195, 416.
62. Yerofeev, B. V. *Dokl Ada Nauk SSSR* 1946, 52, 511.
63. Avrami, M. *J Chem Phys* 1939, 7, 1103; *ibid* 1940, 8, 212; 1940; *ibid* 1941, 9, 177.
64. Cebe, P. *Polym Eng Sci* 1988, 28, 1192; *Polymer* 1986, 2, 1183.
65. Phillips, R.; Manson, J-A. E. *J Polym Sci B: Polym Phys* 1997, 35, 875.
66. Tobin, M. C. *J Polym Sci Polym Phys Ed* 1974, 12, 399.
67. Mandelkern, L. *Crystallization of Polymers*; McGraw Hill Book Company; New York, 1964.
68. Kim, T. K.; Kim, S. O.; Chung, I. J. *Eur Polym J* 1997, 33, 1613.
69. Othman, A.; Tahon, K.; Osman, M. A. *Phys. B Cond Matter* 2002, 311, 356.
70. Sharples, A. *Introduction to Polymer Crystallization*; Edward Arnold; London, 1966.
71. Sajkiewicz, P. *J Polym Sci Part B Polym Phys* 2002, 40, 1835.
72. Yasuda, H.; Olf, H.; Crist, B.; Camaze, C. E.; Peterlin, A. *Water Structure at the Water-Polymer Interfaces*, Plenum Press: New York, 1979; Edn P.35.
73. Gan, Y. S.; Francois, J.; Guenet, J. M.; Gauthier-Manuel, B.; Allain, C. *Makromol Chem Rapid Commun* 1985, 6, 225.
74. Guenet, J. M. *Macromolecules* 1986, 19, 1960.
75. Klein, M.; Guenet, J. M. *Macromolecules* 1989, 22, 3716.